

Finite element analysis of forces on a plane soil blade¹

L. CHI and R. L. KUSHWAHA

¹CSAE paper no. 88-205, Presented at Agricultural Institute of Canada Annual Conference, 21-24 August 1988, Calgary, AB. Department of Agricultural Engineering, University of Saskatchewan, Saskatoon, SK, Canada, S7N 0W0. Received 26 September 1988, accepted 17 April 1989.

Chi, L. and Kushwaha, R. L. 1989. **Finite element analysis of forces on a plane soil cutting blade.** Can. Agric. Eng. 31: 135-140. A non-linear 3-D finite element model was developed to predict the soil forces on a tillage tool. The weighted residual method was applied to formulate the finite element model. The Duncan and Chang hyperbolic stress-strain model was used in the analysis. A FORTRAN program was written to conduct the finite element analysis. The reaction force was obtained from the failure zone calculated by the finite element model. The comparison between the finite element model and two previous models was reasonably good.

INTRODUCTION

Generally all agricultural soil-cutting tools have been developed by field experiment and by trial and error. Because a large amount of energy is consumed during tillage, it is essential to pursue every means toward more efficient design of tillage tools based upon theoretical principles and their efficient operation.

Initially, the theoretical approach to the soil-cutting problem was based on the Terzaghi's passive earth pressure theory. Reece (1965) proposed a fundamental equation for two-dimensional soil failure with a wide cutting blade. Based on this equation, several models were developed for narrow cutting blades (Hettiaratchi and Reece 1967; Godwin and Spoor 1977; McKeyes and Ali 1977; Perumpral et al. 1983).

As computers became more and more accessible, numerical methods were also developed to solve the soil-cutting problem. Yong and Hanna (1977) first proposed a finite element model for two-dimensional soil failure with a wide blade. Chi and Kushwaha (1987) developed a three-dimensional finite element model for a narrow cutting blade. The finite element analysis provides not only the soil forces, but also the stress field (Yong and Hanna 1977), displacement field, failure zone and force distribution (Chi and Kushwaha 1987). The finite element method also shows the possibility of solving the soil-cutting problem dynamically.

This paper describes a finite element model for predicting soil forces. The results obtained from the finite element model were compared with some previous models.

PROCEDURE

Development of the finite element model

The mathematical model of soil cutting can be obtained by taking a small element of soil. The partial differential equations for this element were derived by Harr (1966), which can be expressed in a matrix form as follows:

$$D^T \sigma - f = 0 \quad (1)$$

where:

- D = differential operator matrix.
- σ = stress vector $\{\sigma_x, \sigma_y, \sigma_z, \tau_{xy}, \tau_{yz}, \tau_{xz}\}^T$.
- f = body force vector $\{0, 0, -\gamma\}$.

The stress-strain relationship of soil is a nonlinear. The incremental method was used in the finite element analysis, in which the change in displacement is still very small in each small increment. The difference in strain at each increment can be considered as infinitesimal strain. Therefore, for each increment a linear relationship between strain and displacement is considered but with stiffness varying with total strain. The governing Eq. 1 can be rewritten for each increment in the following form:

$$D^T \sigma_o - D^T C D \Delta u - f = 0 \quad (2)$$

where:

- σ_o = initial stress vector at each increment.
- C = constitutive matrix.
- Δu = incremental displacement change vector.

The exact theoretical solution of Eq. 2 is usually unavailable. The finite element method is a technique for obtaining an approximate solution. A variational statement of finite element formulation is given by the following equation:

$$\int_{\Omega_e} v^T \{D^T \sigma_o - D^T C D \Delta \bar{u} - f\} d\Omega_e = 0 \quad (3)$$

where:

- $\Delta \bar{u}$ = an approximation of displacement vector Δu .
- v = a weighting vector.

Equation 3 shows that the approximate function from finite element method will satisfy the governing differential equations (Eq. 2) in the sense of weighted average for every small element. By integrating Eq. 3 by parts once and rearranging the terms, the following equation was obtained:

$$\int_{\Omega_e} (Dv)^T C D \Delta u d\Omega_e = \int_{\Omega_e} (Dv)^T \sigma_o d\Omega_e + \int_{\Omega_e} v^T f d\Omega_e - \int_{\Gamma} v^T p d\Gamma \quad (4)$$

where p is the surface compression vector. Three components of surface compression vector are shown in Fig. 1. If the v in the Eq. 4 is an arbitrary admissible displacement vector, Eq. 4 is also known as the "principle of virtual work".

The Galerkin method was used to choose the approximation vector $\Delta \bar{u}$ and the weighting function v in Eq. 4. The approximation vector was proposed as a function of the nodal displacement and the weighting vector was assumed to have a similar form as the approximation vector, as shown below:

$$\Delta u^e = \Phi \Delta u_j^e \quad (5)$$

$$v^e = \Phi \beta \quad (6)$$

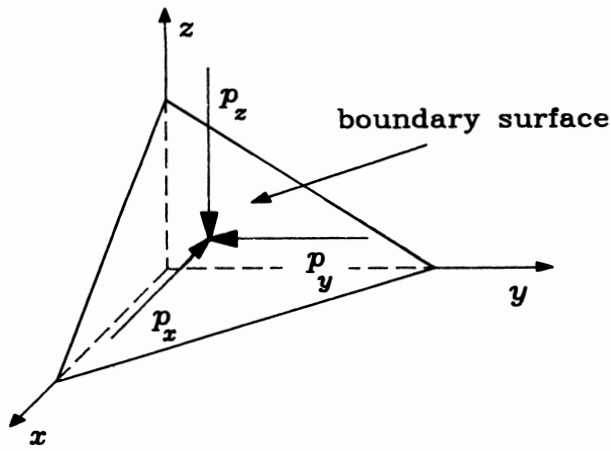


Figure 1. The surface compression on the boundary surface.

where:

- E_t = tangent modulus of soil.
- c = cohesion of soil.
- ϕ = internal friction angle of soil.
- P_a = atmospheric pressure.
- σ_1 = major principal stress.
- σ_3 = minor principal stress.
- R_f = failure ratio.
- K, n = dimensionless numbers.

In Duncan's equation, the tangent modulus E_t of soil was expressed as a function of major and minor principle stresses. The failure ratio R_f in Eq. 9 was defined as the ratio of ultimate deviatoric stress to the soil strength. This tangent modulus E_t and the Mohr-Coulomb failure criterion were utilized in this model. The constitutive matrix is given by the following equation:

$$C = \frac{E_t}{(1+\nu)(1-2\nu)} \begin{pmatrix} 1-\nu & \nu & \nu & 0 & 0 & 0 \\ \nu & 1-\nu & \nu & 0 & 0 & 0 \\ \nu & \nu & 1-\nu & 0 & 0 & 0 \\ 0 & 0 & 0 & \frac{1-2\nu}{2} & 0 & 0 \\ 0 & 0 & 0 & 0 & \frac{1-2\nu}{2} & 0 \\ 0 & 0 & 0 & 0 & 0 & \frac{1-2\nu}{2} \end{pmatrix} \quad (10)$$

where

Δu_j^e = nodal displacement of the element.

Φ = the element shape function.

β = a vector of arbitrary constants.

Substituting Eq. 5 and Eq. 6 into Eq. 4, we will have:

$$\int_{\Omega_e} (D\Phi)^T C D \Phi \Delta d\Omega u_{ej}^e = \int_{\Omega_e} (D\Phi)^T \sigma_o d\Omega_e + \int_{\Omega_e} \Phi^T f d\Omega_e - \int_{\Gamma_e} \Phi^T p d\Gamma_e \quad (7)$$

or

$$K^e \Delta u_j^e = F^e \quad (8)$$

where K^e is element stiffness matrix and F^e is element load vector. The element load vector includes initial stress term, body force term, and the surface compression term.

The constitutive relationship of soil

As the soil is a nonlinear stress-strain material, the E modulus changes with the state of stress. Kondner (1963) proposed a hyperbolic model to represent a typical stress-strain relationship of the soil. Duncan and Chang (1970) developed an equation of the tangent modulus E_t based upon the Kondner's model, which is given below:

$$E_t = \left[1 - \frac{R_f (1 - \sin \phi) (\sigma_1 + \sigma_3)}{2 c \cos \phi + 2 (\sigma_3 + P_a) \sin \phi} \right]^2 K P_a \left[\frac{\sigma_3 + P_a}{P_a} \right]^n \quad (9)$$

where:

ν = Poisson's ratio.

The agricultural soil characteristics lie between sand and pure clay. The two dimensionless parameters selected for the model (Eq. 9) were based on the previous research (Janbu 1963). The value of these parameters are given in Table I.

Finite element mesh

The tetrahedral constant strain elements were used during the analysis because of their simplicity and convenience for analysis of nonlinear material and large displacements, as shown in Fig. 2. The displacement within the element was a linear function as expressed by the following equation:

$$u(x,y,z) = A_0 + A_1x + A_2y + A_3z \quad (11)$$

where:

- $u(x,y,z)$ = the element displacement in the x direction.
- A_i = the coefficients.

An element generating program was written in order to overcome the difficulty of generating the tetrahedral elements. The elements were generated by rectangular prism boxes and each rectangular prism box was divided into six tetrahedral elements, as shown in Fig. 3.

Table 1. Parameters and soil properties used during the finite element analysis and comparison

Terms	Value
Cohesion of soil (c)	10 kPa
Internal friction of soil (ϕ)	30°
Soil density (γ)	15 kN/m ³
External friction (δ)	0 (smooth blade)
Poisson's ratio (ν)	0.48
Failure ratio (R_f)	0.90
K	40
n	0.4
Rake angle (α)	45°, 60°, 90°
Tool depth (d)	10, 20 cm
Tool width (w)	5 cm

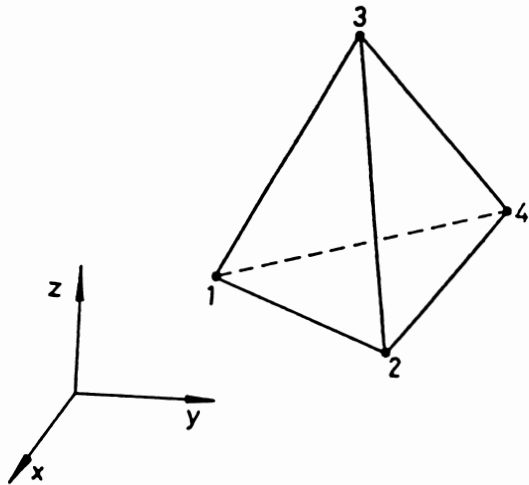


Figure 2. Constant strain tetrahedral element.

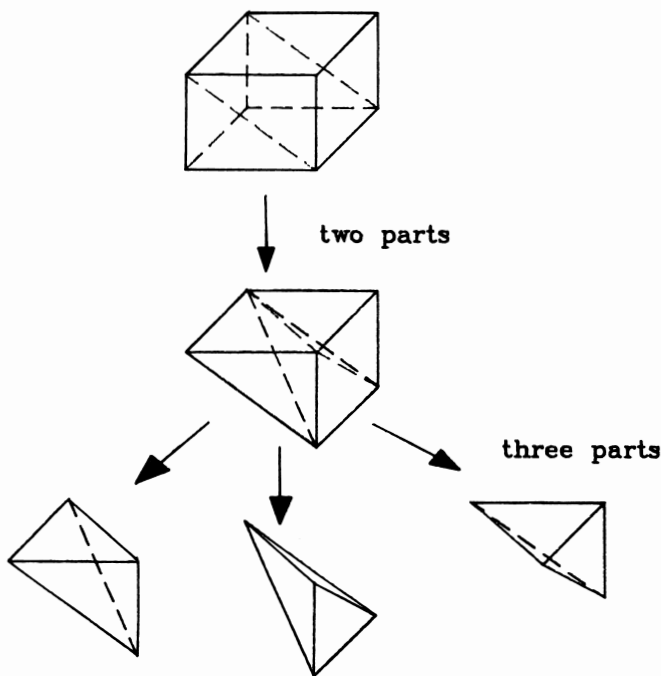


Figure 3. Tetrahedral element generation.

Figure 4 gives the finite element mesh for a narrow vertical blade. The soil failure for a narrow blade is symmetric about the center line of the blade. Thus only half of the total region

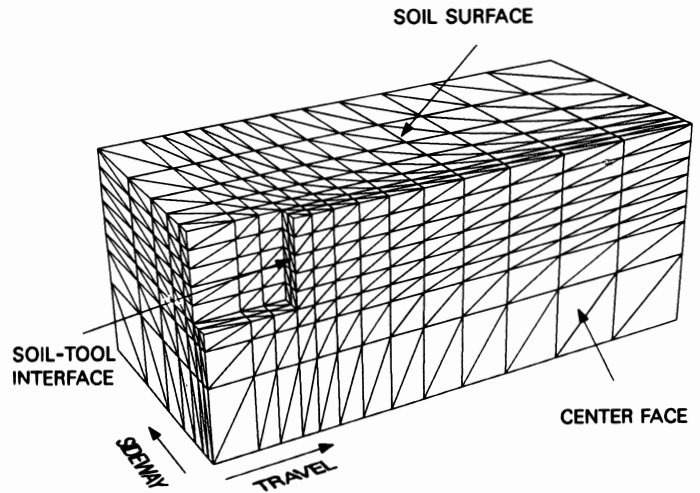


Figure 4. The finite element mesh of a vertical blade showing half zone of influence.

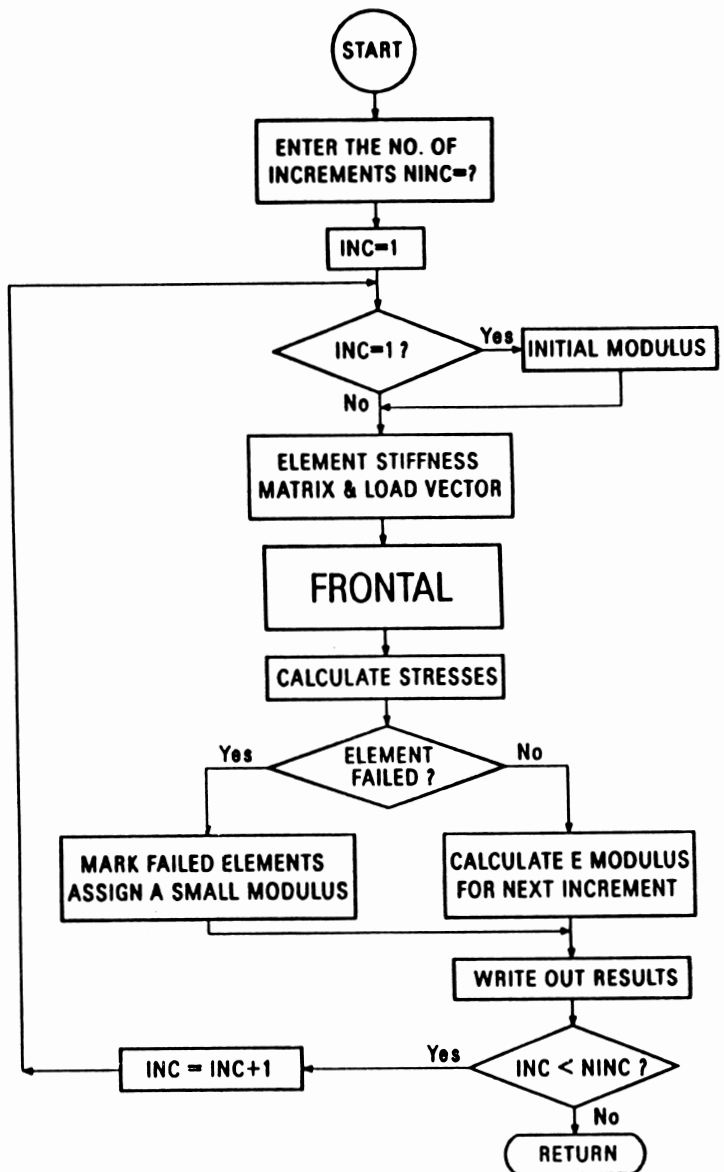


Figure 5. The flow chart of finite element routine.

was considered in the analysis. The region of influence considered in the analysis had a length six times that of the tool operating depth (one tool operating depth behind the tool and five tool operating depths ahead of the tool), a depth 2.5 times that of the tool operating depth and a width six times that of the half tool width. Because of the symmetry, no side movement occurred at the center face (Fig. 4). A total of 978 nodes and 4188 elements were used for a vertical blade.

Computer program

A FORTRAN program was written to conduct the analysis. The program was composed of three parts: (1) data generating, (2) finite element routine, and (3) postprocessing. The data-generating routine was written to generate nodes, elements, boundary, and loading condition. The finite element routine conducted the main parts of analysis. The postprocessing routine was written to calculate total forces, plot the soil failure and soil movement and so on. The finite element analysis was conducted on a VAX/VMS 8650 computer.

Figure 5 gives the flow chart of the finite element routine. The total load was divided into a number of small increments. The tangent modulus E_t was calculated according to the stress level of the element using Eq. 9. The program "FRONTAL" (Irons 1970) assembles the system's stiffness matrix and solves for the displacements and the forces on the interface nodes. The element stresses were accumulated at each increment. The stresses of each element were examined by using the Mohr-Coulomb soil failure theory. The element was indicated failed when its deviatoric stress exceeded the soil strength. A small modulus ($10^{-4} E_t$) was assigned to these failed elements to continue program processing. The nodal coordinates were updated after each increment. The loading was continued until all the soil element ahead of the tool had failed.

RESULTS AND DISCUSSION

At each increment, the reaction forces were calculated from the finite element analysis from a small displacement assigned to the nodes on the interface. Since only half of total region was considered in the analysis, the total draft and vertical force were twice the magnitude obtained from finite element analysis. The total side force on the blade was equal to zero because of the symmetry.

Figure 6 shows the theoretical draft force and displacement curve for a vertical smooth blade 5 cm wide operating at a depth of 10 cm. The draft force increased with the displacement (Fig. 6), and after a number of increments, a small force increment caused a large displacement. This was considered as failure of the soil structure.

At each increment, the element was examined by the Mohr-Coulomb failure criterion and the failed element was marked. It was found that the initial soil failure started around the bottom of the tool. As the load increased, failure region extended around the tool edge and towards the soil surface. Figure 7 shows the soil failure in x - z plane which occurred at increment No. 26. The failed element was identified by a cross in the diagram. A complete failure region from the tip of tool to the soil surface was formed at increment No. 26, as shown in Fig. 7. This was defined as failure point of the soil column (Fig. 6) and the corresponding force was considered as the soil reaction force required to cut the soil.

The value of tangent modulus of the soil from the hyperbolic model will approach zero as the strain increases. A zero modulus was not acceptable to continue the finite element analysis program.

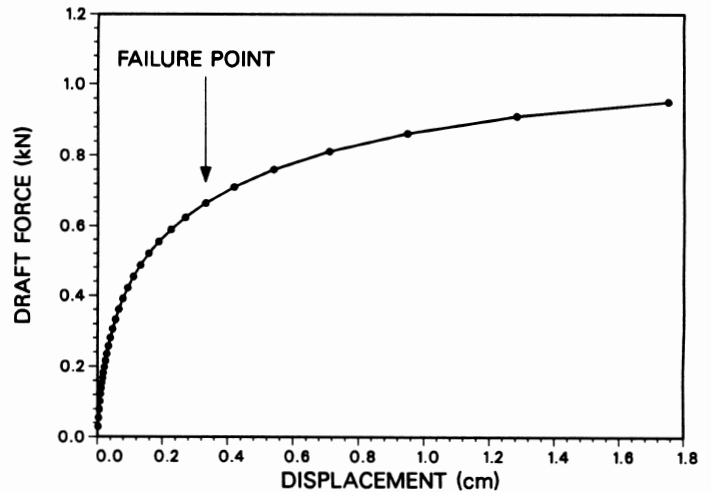


Figure 6. Draft force of a smooth vertical blade, $d = 10$ cm, $w = 5$ cm.

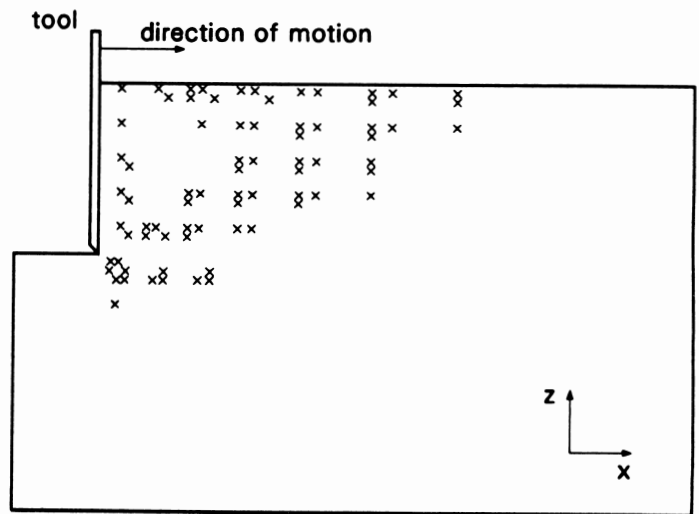


Figure 7. The soil failure (x) of a smooth vertical blade at increment No. 26.

Thus, a small residual modulus was assigned to the element when the deviatoric stress of the element exceeded the shear strength of the soil. Because of this residual modulus, the reaction forces continued to increase with the displacement after the soil structure had failed.

The results obtained from the finite element method were compared with the McKyes and Ali (1977) and Perumpral et al. (1983) model, as shown in Figs. 8 and 9. The draft force of the previous model was calculated based on the procedure described by McKyes and Ali (1977) and Perumpral et al. (1983). The comparison between finite element model and the two other models were reasonably in agreement. The three results were very close at a rake angle of 60° . For the model of McKyes and Ali (1977), at a rake angle of 45° , the optimized angle between the soil surface and the bottom plane of failure wedge was close to extreme condition (90°), which resulted in a small predicted draft force. At a rake angle of 45° , the results from the finite element method were close to the model of Perumpral et al. (1983). For a vertical blade, the results of the finite element model were between the two models. The model of Perumpral et al. (1983) produced a relatively lower draft prediction for the vertical blade.

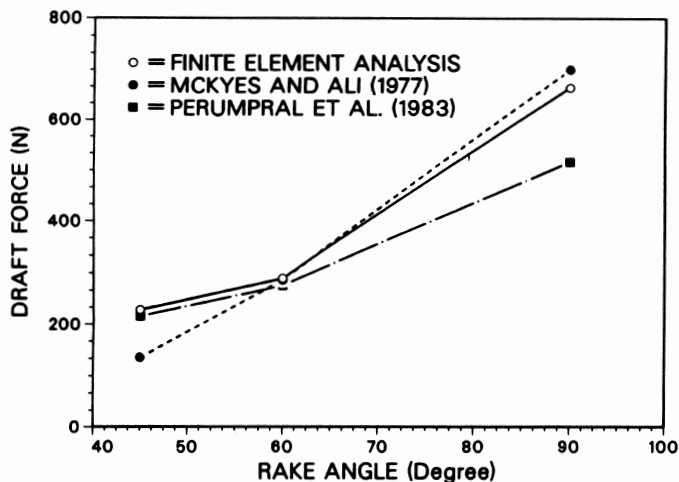


Figure 8. Comparison of the finite element model with previous models, $d = 10$ cm, $w = 5$ cm.

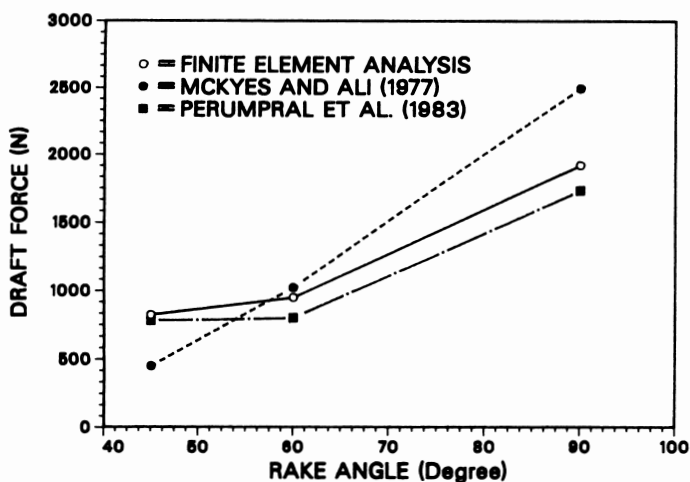


Figure 9. Comparison of the finite element model with previous models, $d = 20$ cm, $w = 5$ cm.

The force distribution along the tillage tool can also be obtained from the finite element analysis. Figure 10 shows the predicted draft force distribution for a 5-cm-wide smooth vertical blade operating at a depth of 10 cm. The theoretical force on the tool edge was found to be larger than the force at the center of the tool (Fig. 10). The force also increased with the increase in depth, with the maximum force occurring at the outer edges of the tool at the bottom.

CONCLUSION

A three-dimensional finite element model was developed for the analysis of soil forces on a narrow tillage tool. This finite element model was used to study soil reaction forces, soil failure pattern, soil movement and force distribution.

The reaction force increased with the increase in displacement of the tool in the direction of travel. The reaction forces were obtained from the failure zone calculated by the finite element model. Soil failure started from the tool tip and extended toward the soil surface with measuring tool movement. At a complete failure of the soil profile, the corresponding reaction force was taken as the required force for soil cutting.

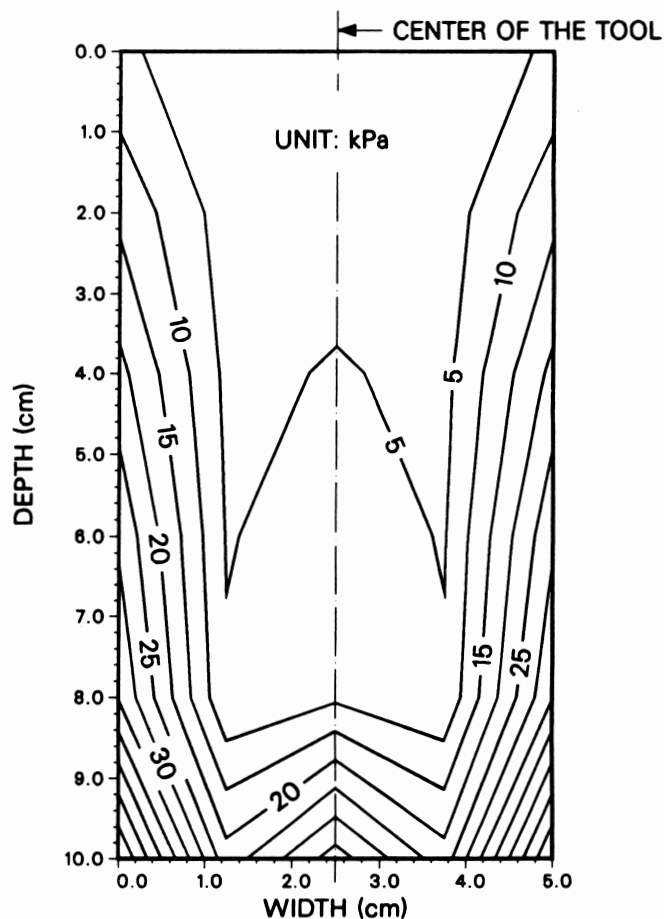


Figure 10. The soil stress distribution on a smooth vertical blade.

The comparison between the finite element model draft force prediction and those of two previous models was reasonably good.

The stress distribution obtained from the finite element analysis showed that the maximum stress occurred at the tip of the tool.

REFERENCES

- CHI, L. and R. L. KUSHWAHA. 1987. Three-dimensional finite element analysis of soil failure under a narrow tillage tool ASAE Paper No. 88-1582, Trans. Am. Soc. Agric. Engrs., St. Joseph, MI.
- DUNCAN, J. M. and C. Y. CHANG. 1970. Nonlinear analysis of stress and strain in soil. J. Soil Mech. and Foundations Div., Proc. of Am. Soc. Civ. Engrs. 96(SM5): 1629-1653.
- GODWIN, R. J. and G. SPOOR. 1977. Soil failure with narrow tine. J. Agric. Eng. Res. 22: 213-228.
- HARR, M. E. 1966. Foundation of theoretical soil mechanics. McGraw-Hill Book Company, New York, NY.
- HETTIARATCHI, D. R. P. and A. R. REECE. 1967. Symmetrical three-dimensional soil failure. J. Agric. Eng. Res. 4: 45-67.
- IRONS, B. M. 1970. A frontal solution program for finite element analysis. Int. J. for Num. Meth. Eng. 2: 5-32.
- JANBU, N. 1963. Soil compressibility as determined by oedometer and triaxial test. European Conference on Soil Mech. and Found. Eng., Wiesbaden, Federal Republic of Germany, Vol. 1, pp. 19-25.
- KONDER, R. L. and J. S. ZELASKO. 1963. A hyperbolic stress-strain response: cohesive soil. J. Soil Mech. Found. Div. Am. Soc. Civ. Engrs. 89(SM1): 115-143.
- MCKYES, E. and O. S. ALI. 1977. The cutting of soil by narrow blade. J. Terramechan. 14(2): 43-58.

PERUMPRAL, J. V., C. S. GRISSO, and C. S. DESAI. 1983. A soil-tool model based on limit equilibrium analysis. *Trans. Am. Soc. Agric. Engrs.* 26: 991-995.

REECE, A. R. 1965. The fundamental equation of earth-moving mechanics. *Symposium on earth-moving machinery.*

Proceedings of the Institute of Mechanical Engineers. 179 Part 3F: 16-22.

YONG, R. N. and A. W. HANNA. 1977. Finite element analysis of plane soil cutting. *J. Terramechan.* 14: 103-125.